Comparison of Density Wave Oscillation Onset under Uniform and Representative HSG Heat-Flux Profiles using MARS-KS

Jun Ha Hwang [a], Jeong Ik Lee [a*]
[a]*Department of Nuclear and Quantum Engineering, Korea Advanced Institute of Science and Technology, 373-1 Guseong-dong Yuseong-gu, Daejeon 305-701, Republic of Korea*
[*]*Corresponding author: jeongiklee@kaist.ac.kr*

***Keywords :** Helical Steam Generator, MARS-KS, Heating Profile, Density Wave Oscillation, Instability

1. Introduction

As global demand for decarbonization continues to increase, nuclear energy is receiving renewed attention as a reliable low-carbon energy source. In particular, advanced reactors are being developed with an emphasis on system simplification, modularization, and compactness, which requires improved performance and integration of major components. Helical steam generators (HSGs) can provide a large heat-transfer area within a limited volume and are therefore advantageous for improving the compactness of advanced reactor systems. However, their helical geometry and once-through operation result in thermal-hydraulic behavior that differs from that of conventional U-tube steam generators.

One of the important thermal-hydraulic phenomena in HSGs is density wave oscillation (DWO). DWO is a dynamic two-phase flow instability in which a perturbation in channel flow rate changes the heat input per unit mass, boiling boundary, phase-change region, void fraction, and pressure-drop response, which in turn feeds back to the flow rate. In parallel channels, the common inlet and outlet header conditions can further couple the pressure-drop response of individual channels with flow redistribution, resulting in out-of-phase oscillations between channels.

Uniform heat flux is often assumed in DWO analyses to simplify the problem. In an actual HSG, however, the heat flux transferred to the secondary side can vary along the axial direction due to changes in the temperature difference between the primary and secondary sides, heat-transfer coefficients, flow arrangement, and phase-change process. Even at the same total heat input, differences in the axial heat-flux profile can affect the location of the boiling boundary, length of the phase-change region, outlet quality, pressure-drop components, and time-delayed response to flow perturbations.

In this study, the DWO thresholds obtained under the two heat-flux conditions are compared, and the effect of the axial heat-flux distribution on flow stability is discussed. The results provide guidance for selecting appropriate heat-flux assumptions in future HSG DWO stability analyses.

2. Methodology

2.1 Detection of DWO

To evaluate the DWO onset and construct the stability boundary, the dimensionless stability map proposed by Ishii and Zuber, as shown in Figure 1, was used [1]. The subcooling number (N_{sub}) and phase-change number (N_{pch}) are defined by Equation (1) and (2), respectively, using thermodynamic properties evaluated at the system outlet pressure.

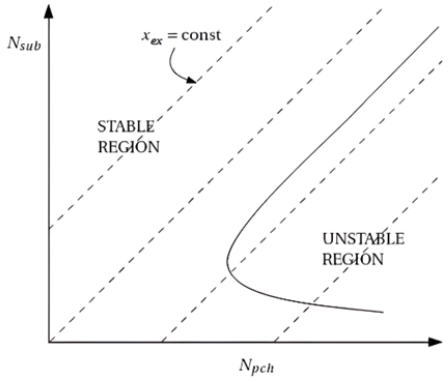

Fig. 1. Stability map

$$N_{sub} = \frac{\Delta h_{in}}{h_{fg}} \frac{\rho_{fg}}{\rho_g} \quad (1)$$

$$N_{pch} = \frac{\mathrm{Q}}{\dot{m} h_{fg}} \frac{\rho_{fg}}{\rho_g} \quad (2)$$

For each N_{sub}, the heating rate was increased stepwise while maintaining the inlet mass flow rate and temperature. Sufficient time was allowed after each step to reach a quasi-steady condition. The onset of DWO was identified when sustained flow oscillations were observed. For the parallel-channel configuration, the out-of-phase oscillation of the two channel flow rates was used as the main indicator of DWO onset as shown in Figure 2. The corresponding N_{pch} was then used to define the stability boundary.

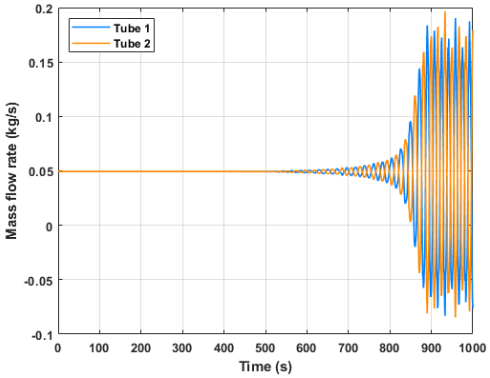

Fig. 2. Mass flow rate change over time.

2.2 Code Implementation

Pressure drop is an important parameter for predicting the onset of density wave oscillation (DWO) in helical tubes. However, the standard MARS-KS 2.0 code does not include a frictional pressure drop model specifically for helical geometries. In this study, the modified MARS-KS code developed by Oh (2024) was used[2]. The code incorporates the Ito model for single-phase flow and the Colombo model for two-phase flow, as shown in Equation (3) and (4), respectively, to calculate the frictional pressure drop in helical tubes[3, 4].

$$f\left(\frac{D}{d}\right)^{\frac{1}{2}} = 0.029 + 0.304\left[Re\left(\frac{d}{D}\right)^{2}\right]^{-0.25} \quad (3)$$

$$\Phi_{\mathrm{l}}^{2} = 0.0986\left(1 + \frac{20}{x_{tt}} + \frac{1}{X_{tt}^{2}}\right) De_{l}^{0.19}\left(\frac{\rho_m}{\rho_l}\right)^{-0.4} \quad (4)$$

2.3 Reference Helical Steam Generator

The helical coil geometry was based on publicly available design data for the SMART (System-integrated Modular Advanced Reactor) steam generator. The geometric parameters and boundary conditions used to reproduce the heat flux distribution are summarized in Table I.

To simplify the comparison of DWO behavior, the original 376-tube configuration was reduced to two parallel tubes, and the primary-side flow area was scaled to match the flow assigned to each tube. The coil diameter and length were based on the ninth layer, which is the middle layer of the 17-layer SMART steam generator.

Several thermal-hydraulic conditions were adjusted for the analysis, including the feedwater temperature and primary-side flow rate. Orifice throttling was not applied because it can suppress DWO and obscure the effect of the heat flux distribution on the instability threshold. On the secondary side, the inlet temperature was varied to obtain different subcooling numbers for the stability map. The primary-side flow rate was then increased to raise the heat transfer rate and obtain higher phase-change numbers.

Table I: SMART Helical Tube Geometry

Tubes per SG	376	
Tube Specifications	Material	Inconel 690
	Inner diameter [mm]	12
	Outer diameter [mm]	17
	Coil diameter [m]	0.937
	Tube length [m]	25.42
	Inclination angle [°]	8.5
	Effective height [m]	3.8
Primary side	Pressure [MPa]	15.0
	Inlet temperature [K]	596.15
	Outlet temperature [K]	568.85
	Mass flow rate [kg/s]	261.25
Secondary side	Pressure [MPa]	5.2
	Inlet temperature [K]	473.15
	Outlet temperature [K]	>569.15
	Mass flow rate [kg/s]	20.1

2.4 MARS-KS Modelling

The modeling approach using the modified MARS-KS code is shown in Figure 3. For the uniform heat flux case, two helical tubes connected to common inlet and outlet headers were modeled using PIPE components with specified inclination angles. Helical-coil heat transfer and pressure drop models were applied to the corresponding heat structures. A constant heat input was imposed on the tube heat structures using predefined tables.

For the non-uniform heat flux case, the primary side was modeled as a vertically downward-flowing PIPE, with the flow area based on the ninth layer of the helical coil (Figure 4). The primary and secondary sides were thermally coupled through heat structures to reproduce the axial heat flux distribution of the steam generator (Figure 5).

Stability maps were generated at subcooling numbers of 2, 4, 6, 8, and 10. For the uniform heat flux cases, the total heating power was increased in 2 kW increments. For the non-uniform cases, the primary-side mass flow rate was increased in 0.005 kg/s increments to increase the heat transfer rate. In both cases, the phase-change number was calculated using the total heat transferred to the secondary side at each quasi-steady condition, so that the stability boundaries could be compared on the same dimensionless basis. Sufficient time was allowed after each change to reach a quasi-steady state.

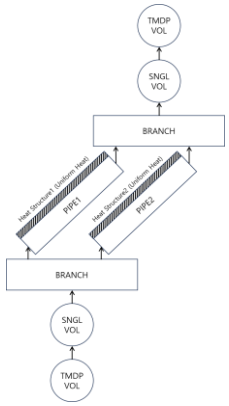

Fig. 3. Nodalization for the uniform heat flux case

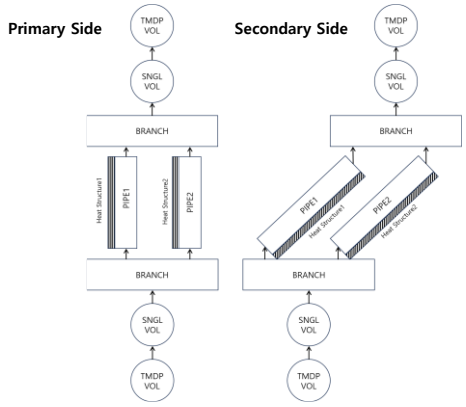

Fig. 4. Nodalization for the non-uniform heat flux case

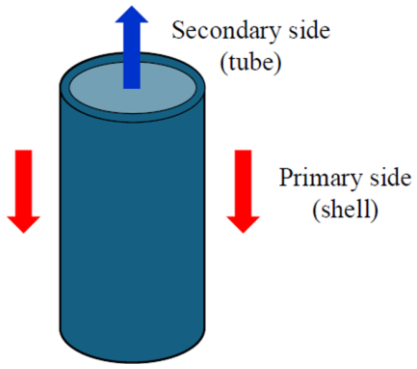

Fig. 5. Heat structure conjunction

3. Result and Discussion

The DWO onset characteristics were compared between the uniform and non-uniform heat flux conditions based on the calculated axial heat flux distributions and stability boundaries. As shown in Figure 6, the axial heat input profile at DWO onset for the representative HSG case exhibits a concave distribution, with lower heat input near the middle of the tube than near the inlet and outlet. In the present calculations, DWO onset was predicted before the channel reached a post-dryout condition.

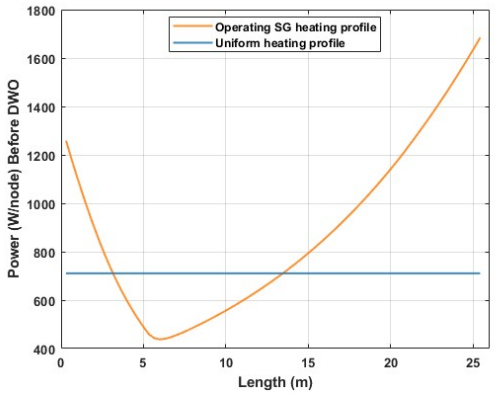

Fig. 6. Axial heat input profiles before DWO onset under uniform and representative HSG heating conditions

The effect of the heating profile on the DWO stability boundary is shown in Figure 7. The stability map is defined by the subcooling number, N_{sub}, and the phase-change number, N_{pch}. For the same N_{sub}, the uniform heating condition predicts DWO onset at a lower N_{pch}, corresponding to a lower heating power, than the representative HSG heating profile. This indicates that the uniform heating assumption gives a more conservative prediction of the DWO threshold in the present cases.

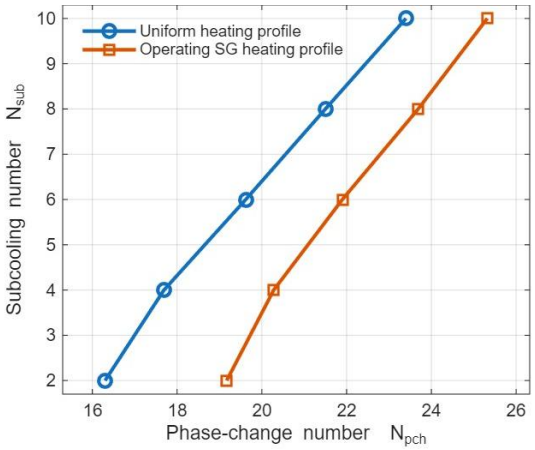

Fig. 7. Comparison of stability map under uniform and non-uniform heating conditions

To examine the origin of the stability-boundary shift, the axial vapor-generation distributions before DWO onset are compared in Figure 8. The location where vapor generation starts represents the approximate boiling boundary. Along the stability boundary, the boiling-boundary movement with N_{sub} appears less pronounced for the representative HSG heating profile than for the uniform heating condition. This suggests that the phase-boundary response is moderated when the axial heat input is determined by the coupled primary-to-secondary heat transfer condition.

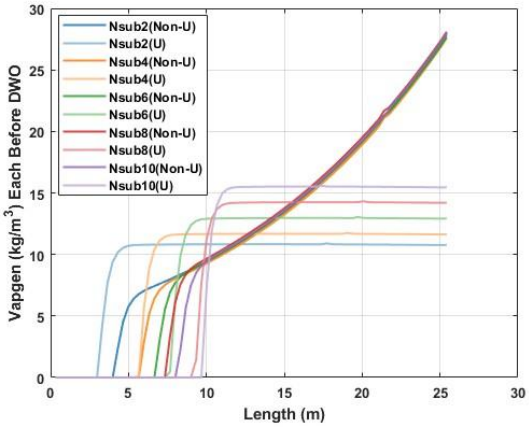

Fig. 8. Axial vapor-generation distributions before DWO onset under uniform and representative HSG heating profiles

In addition to the boiling-boundary behavior shown in Fig. 8, Fig. 9 compares the axial void-fraction distributions before DWO onset at N_{sub} =4. This case was selected because the two heating profiles show similar approximate boiling-boundary locations, allowing the downstream void-fraction development to be compared more clearly. The figure shows that the heating profile changes the void-fraction development downstream of the boiling boundary. Under the uniform heating condition, the void fraction increases more rapidly after boiling begins and remains relatively high over much of the middle section. In contrast, the representative HSG heating profile shows a more gradual and non-uniform void-fraction development, with relatively lower void fraction in the middle section and a stronger increase toward the downstream region. This indicates that the stability-boundary shift is not governed by the boiling-boundary location alone, but by the combined effect of phase-boundary response, void-fraction development, and the resulting delayed pressure-drop response.

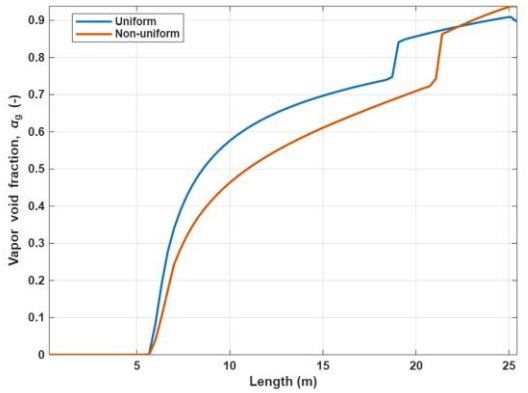

Fig. 9. Axial void fraction distributions before DWO onset for uniform and representative HSG heating profiles at $N_{sub} = 4$

4. Conclusion

This study compared MARS-KS predictions of DWO onset in parallel helical-coiled channels under uniform and representative HSG heating profiles. At the same subcooling number, the uniform heating condition predicted DWO onset at a lower phase-change number than the representative HSG profile. This indicates that the uniform heating assumption provided a more conservative prediction of the DWO threshold for the present calculation conditions.

The axial vapor-generation and void-fraction distributions were examined to interpret the shift in the stability boundary. Along the stability boundary, the boiling-boundary movement with subcooling appeared less pronounced under the representative HSG profile than under the uniform heating condition. In addition, the representative HSG profile produced non-uniform vapor-generation and void-fraction distributions, with relatively lower values in the middle section and increasing values toward the downstream region. These results suggest that the stability-boundary shift is not determined only by the boiling-boundary location, but also by the axial development of vapor generation, void fraction, and the resulting delayed pressure-drop response.

These results suggest that the axial heat-flux profile is an important modeling assumption in HSG DWO stability analysis. Further studies are needed for different operating conditions, orifice-throttling conditions, and validation against experimental data.

REFERENCES

[1] M. Ishii, et al., Thermally induced flow instabilities in two phase mixtures, Intemat. Heat Transfer Confer. 4 (1970).
[2] Oh, S., Kim, D. H., & Lee, J. I. (2024). Prediction of density wave oscillation in helical steam generators using the MARS-KS Code. International Journal of Heat and Mass Transfer, 235, 126226.
[3] H. Ito, Friction factors for turbulent flow in curved pipes, Journal of Basic Engineering 81 (1959) 123–132.
[4] M. Colombo, L. P. M. Colombo, A. Cammi, M. E. Ricotti, A scheme of correlation for frictional pressure drop in steam-water two-phase flow in helicoidal tubes, Chemical Engineering Science 123 (2015) 460–473.
[5] Korea Institute of Nuclear Safety, “MARS-KS Code Manual Volume 5: Models and Correlations Manual”, KINS/RR-1822, 2022.